Supporting Information

Sasidharan et al. 10.1073/pnas.1203306109

SI Materials and Methods

Strains and Genetics. Strains were cultured at 20 °C on OP50 *Escherichia coli*–seeded NGM plates as described previously and according to German laws for *C. elegans* handling (1). The following strains were used in this study: Bristol N2, *unc-31 (e928)*, *unc-108 (n501)*, *rab-3 (js49)*, *rab-6.2 (ok2254)*, *rab-8 (tm2991)*, *rab-10 (ok1494)*, *rab-11.2 (tm2081)*, *rab-14 (tm2095)*, *rab-18 (ok2020)*, *rab-19 (ok1845)*, *rab-21 (ok1879)*, *rab-27 (tm2306)*, *rab-28 (ok3424)*, *rab-33 (ok1561)*, *rab-35 (tm2058)*, *rab-37 (tm2089)*, *rab-39 (tm2466)*, *tbc-2 (qx20)*, *tbc-2 (tm2241)*, *tbc-4 (ok2928)*, *tbc-4 (tm3255)*, *rabn-5 (ok1555)*, *eri-1 (mg366)*, and *rde-4 (ne301)*.

The following are integrated transgenic lines used in this study: nuIs152[punc-129::gfp-snb-1], nuIs168[punc-129::venus-rab-3], nuIs183 [punc129::nlp-21-venus], nuIs195[punc129::ins-22-venus], zxIs5[unc-17::chop-2 (H134R)-yfp;lin-15 (+)] X, zxIs6 [unc-17::chop-2 (H134R)-yfp;lin-15 (+)] IV, bIs34[prme-8::rme-8–gfp], gzsi1[prab-3::mcherry-rab-10], and ceis59 [punc-129::yfp-rab-5].

Newly generated transgenic lines carrying extrachromosomal arrays are listed in Tables S1 and S2. Plasmids designated in Table S2 were mixed to a final concentration of 100 ng/μL along with pbluescript. These mixtures were microinjected into *C. elegans* to generate transgenic lines as described previously (2). Gzsi1 is a single-copy integrant generated using the previously described Mos1-mediated single copy insertion (MOSCI) technique (3).

Molecular Cloning. The *rab-10* gene was PCR amplified from a cDNA library (ProQuest; Invitrogen). For subcellular colocalization, the RAB-10 was N-terminally fused to mCherry/GFP and expressed under the pan-neuronal 1.2-kb *rab-3* promoter. The *tbc-4*, *rabn-5*, *ehbp-1*, and *eea-1* genes were also amplified from the same library. *tbc-4* and *rabn-5* were N-terminally fused with tagRFP/GFP and cloned under the *rab-3* promoter. *ehbp-1* was fused C-terminally with tagRFP and cloned under the same promoter. The following colocalization markers were used for this study: *prab-3::gfp–cytochrome b5*, *prab-3::manosidase II–gfp*, *prab-3::2xfyve domain–gfp*, *prab-3::rfp-ecop*, and *prab-3::tagRFP-syx-6* (4). Another marker, *apt-9*, was also amplified out of the cDNA library, fused C-terminally to YFP and cloned under the *rab-3* promoter.

For RNAi experiments, rab-1, rab-5, rab-6.1, rab-7, rab-10, rab-11.1, rab-30, rab-33, rab-35, rabn-5, eea-1, and ehbp-1 were cloned into the L4440 RNAi feeding vector.

For Y2H experiments, all *C. elegans rab* genes were cloned and mutated via site-directed mutagenesis to generate dominant-active and dominant-negative variants. The following are the list of dominant-active mutations that were introduced: *rab-1 Q70L*, *rab-2 Q65L*, *rab-3 Q81L*, *rab-5 Q78L*, *rab-6.1 Q70L*, *rab-6.2 Q69L*, *rab-7 Q68L*, *rab-8 Q67L*, *rab-10 Q68L*, and *rab-11.1 Q70L*. The following are the list of dominant-negative mutations that were introduced: *rab-1 25N*, *rab-2 S20N*, *rab-3 T36N*, *rab-5 S33N*, *rab-6.1 T25N*, *rab-6.2 T24N*, *rab-7 T23N*, *rab-8 T22N*, *rab-10 T23N*, and *rab-11.1 S25N*. All mutated *rab* genes were cloned into the pGBKT7 vector as bait. The catalytic arginine finger of TBC-4 was mutated to alanine to generate *tbc-4 R155A*. Wild-type *tbc-2 tbc-4*, *tbc-4 (377-825)*, and *tbc-4 R155A* were cloned into pGADT7 as prey. *rabn-5* and *rabn-5 (1-292)* were cloned into both pGBKT7 and the pGADT7.

RNAi. RNAi knockdown was performed via feeding as described previously (5). All genes for RNAi experiments were cloned into L4440 and transformed into *E. coli* HT115 (DE3) strain. The overnight culture grown in Luria broth media was seeded onto NGM plates containing 100 μg/mL ampicillin and 1 mM isopropyl β-D-1-thiogalactopyranoside (IPTG). Ten L4 animals of strains of interest in an *eri-1 (mg366)* background were transferred onto plates and allowed to lay eggs for 12 h. The animals were then transferred to a second round of plates and allowed to lay eggs for another 12 h. Parents were then removed and the progeny was analyzed.

TR-BSA Endocytosis Assay. The endocytosis of the fluid marker (TR-BSA) was monitored as described previously (6). Strains of interest were crossed into the bIs34 strain to label early endosomes. TR-BSA (1 mg/mL) was injected into the pseudocoelom near the pharynx of adult animals. After specific time points (10, 30, and 45 min), animals were transferred onto chilled NGM plates to retard trafficking and prepared subsequently for imaging. Different injected animals were imaged for each time point. At least four animals were used for a specific time point.

Data Analysis. All analyses for Fig. 5 were performed using self-written routines in Matlab (Mathworks). The image frames, obtained at a high-pixel density (pixel size, 10.1 nm), were binned 2×2 to increase the signal-to-noise ratio and were filtered by both median and averaging filters, to further enhance recognition of the organelles. Background was eliminated by automatic thresholding, based on intensity values determined in a background region selected manually by the user. The Pearson's correlation coefficient between the fluorescence signals given by the organelles (excluding background) was then calculated using the *corr2* Matlab function (Fig. 5 *C* and *F*).

To obtain the average organelle images (Fig. 5*E*), we applied a threshold to each green image that eliminated all green background signal, as above. A square region (1.2×1.2 μm) centered on the intensity maximum of each green organelle was then automatically selected in both the green and the red frame. The green/red regions from all identified green organelles ($n = 75$–99, for the different genotypes) were then averaged using an automatic routine in which they were rotated to obtain the best possible signal overlap. Line scans through the averaged regions are presented in Fig. 5.

Y2H Assay. The Matchmaker Y2H assay was performed according to manufacturer's protocol (Clontech). All Rabs were cloned into the bait vector pGBKT7, whereas *tbc-2*, *tbc-4*, *tbc-4 (377-825)*, and *tbc-4 R155A* were cloned into the prey vector pGADT7 (Clontech), respectively. *rabn-5* and *rabn-5 (1-292)* were cloned into both pGBKT7 and the pGADT7. The plasmid combinations of interest were transformed into the yeast strain AH109 (Clontech) and tested for interaction by spotting on selection plates lacking histidine.

Coimmunoprecipitation. COS7 cells were grown in 15-cm-diameter cell culture dishes in DMEM (with 10% FCS, 4 mM glutamine, 100 U/mL each penicillin and streptomycin) at 37 °C at 5% CO_2. RABN-5 was tagged to GFP, and TBC-4 (377–825 aa) was tagged to V5 for expression in mammalian cells. Coimmunoprecipitation (Co-IP) experiments were carried out as described previously (7).

Confocal Microscopy and Image Analysis. Animals were immobilized with 50 mM Na-azide and placed on 2% (wt/vol) agarose pads. All imaging was performed on an inverted confocal microscope (SP2; Leica). Images were taken using a 63× NA 1.32 oil immersion objective at 20 °C. Stacks of regions of interest were taken and then compiled to generate maximum intensity projections using Leica software.

For subcellular localizations, images of neuronal cell somas from the VNC were taken. Images for quantification from DNC and coelomocytes was carried out as described previously (8). Maximum stack projections taken from the confocal software were thresholded and quantified using ImageJ software (National Institutes of Health) as described previously (4). All data were normalized to wild type.

For Fig. 2*D* and Fig. 5, imaging was performed using a TCS STED SP5 system (Leica), with a 100× NA 1.4 objective, as above. Image analysis was performed by self-written routines in Matlab (Mathworks).

High-Pressure Freeze Electron Microscopy. A 100-μm-deep aluminum platelet (Microscopy Services) was filled with *E. coli* OP50 suspension. About 20 young adult worms were transferred into the chamber and immediately frozen using a BalTec HPM 10. Freeze substitution was carried out in a Leica AFS2. Incubations were at −90 °C for 100 h in 0.1% tannic acid, 7 h in 2% OsO_4, and at −20 °C for 16 h in 2% OsO_4, followed by embedding in epoxy resin at room temperature (9) (all solutions wt/vol in dry acetone). Fifty-nanometer sections were mounted on copper slot grids and placed for 10 min on drops of 4% (wt/vol) uranyl acetate in 75% methanol and then washed in distilled water. After air drying, the grids were placed on lead citrate (10) for 2 min in a CO_2-free chamber and rinsed in distilled water. Micrographs were taken with a 1024 × 1024 CCD detector (Proscan CCD HSS 512/1024; Proscan Electronic Systems) in a Zeiss EM 902A, operated in the bright field mode.

Electrophysiology. Recordings from dissected *C. elegans* body-wall muscle cells were conducted as described previously (11). After dissection, cells were treated for 8 s with 0.5 mg/mL collagenase (Sigma-Aldrich) in modified Ascaris Ringer's (AR) [150 mM NaCl, 5 mM KCl, 5 mM $CaCl_2$, 1 mM $MgCl_2$, 10 mM glucose, 15 mM Hepes (pH 7.35), 340 mOsm] and washed with AR. Cells were clamped to a holding potential of −60 mV using an EPC10 amplifier and analyzed by Pulse software (HEKA Electronics). The bath solution was AR, and the pipette solution was 120 mM KCl, 20 mM KOH, 4 mM $MgCl_2$, 5 mM Tris-HCl (pH 7.2), 0.25 mM $CaCl_2$, 4 mM ATP, 36 mM sucrose, and 5 mM EGTA (315 mOsm). Light activation was performed using a LED lamp (KSL-70; Rapp OptoElectronic) at a wavelength of 470 nm (8 mW/mm^2) and controlled by the HEKA amplifier software.

1. Brenner S (1974) The genetics of Caenorhabditis elegans. *Genetics* 77:71–94.
2. Mello CC, Kramer JM, Stinchcomb D, Ambros V (1991) Efficient gene transfer in C.elegans: Extrachromosomal maintenance and integration of transforming sequences. *EMBO J* 10:3959–3970.
3. Frøkjaer-Jensen C, et al. (2008) Single-copy insertion of transgenes in Caenorhabditis elegans. *Nat Genet* 40:1375–1383.
4. Sumakovic M, et al. (2009) UNC-108/RAB-2 and its effector RIC-19 are involved in dense core vesicle maturation in Caenorhabditis elegans. *J Cell Biol* 186:897–914.
5. Kamath RS, Martinez-Campos M, Zipperlen P, Fraser AG, Ahringer J (2001) Effectiveness of specific RNA-mediated interference through ingested double-stranded RNA in Caenorhabditis elegans. *Genome Biol* 2: RESEARCH0002.
6. Zhang Y, Grant B, Hirsh D (2001) RME-8, a conserved J-domain protein, is required for endocytosis in Caenorhabditis elegans. *Mol Biol Cell* 12:2011–2021.
7. Hannemann M, et al. (2012) TBC-8, a putative RAB-2 GAP, regulates dense core vesicle maturation in Caenorhabditis elegans. *PLoS Genet* 8:e1002722.
8. Sieburth D, Madison JM, Kaplan JM (2007) PKC-1 regulates secretion of neuropeptides. *Nat Neurosci* 10:49–57.
9. Rostaing P, Weimer RM, Jorgensen EM, Triller A, Bessereau JL (2004) Preservation of immunoreactivity and fine structure of adult C. elegans tissues using high-pressure freezing. *J Histochem Cytochem* 52:1–12.
10. Reynolds ES (1963) The use of lead citrate at high pH as an electron-opaque stain in electron microscopy. *J Cell Biol* 17:208–212.
11. Liewald JF, et al. (2008) Optogenetic analysis of synaptic function. *Nat Methods* 5: 895–902.

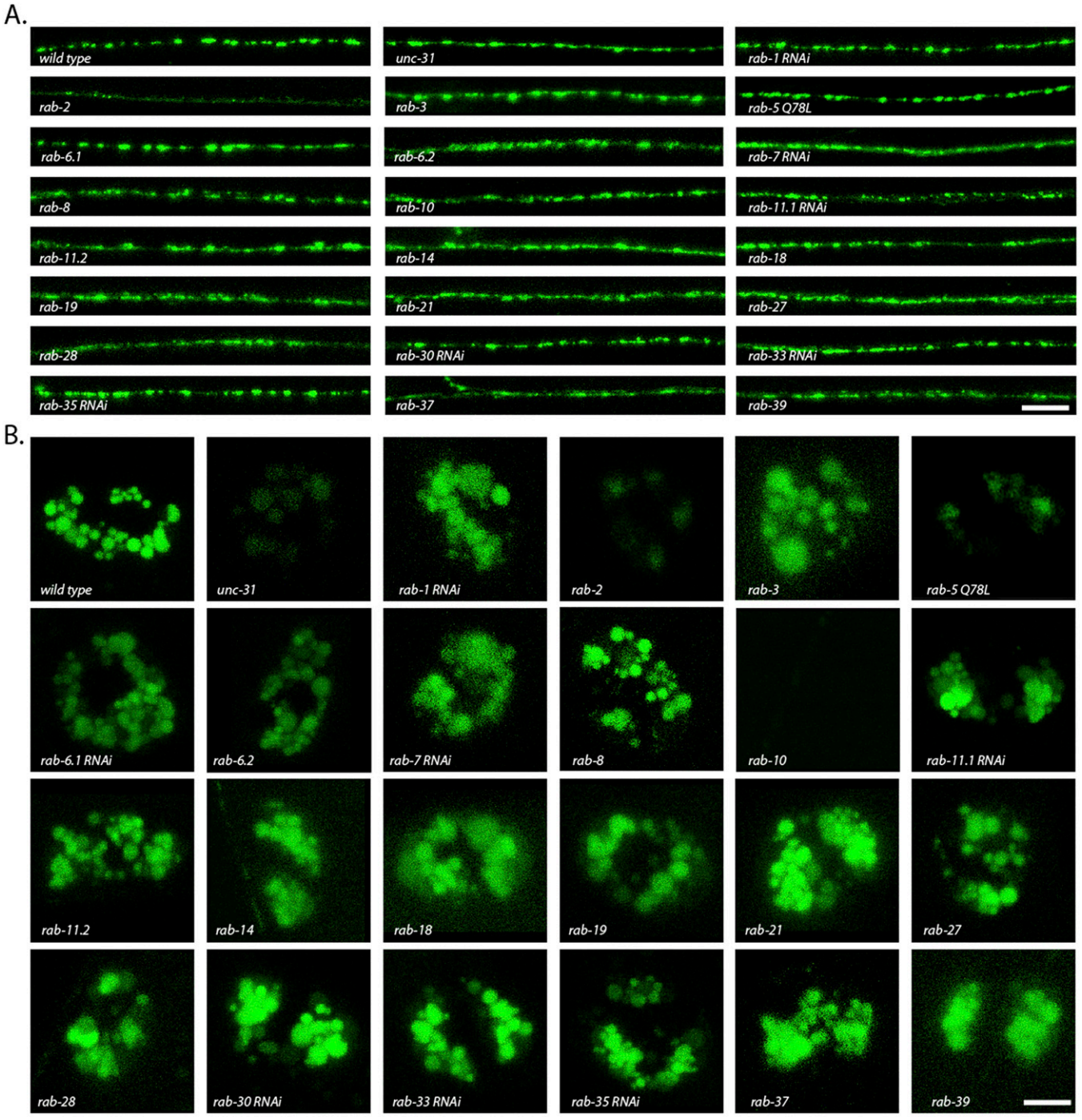

Fig. S1. Systematic analysis of all *C. elegans* RABs to identify regulators of DCV secretion. All available *rab* mutants were tested for defects in NLP-21-YFP secretion. For Rabs where no mutant was available, tissue-specific knockdown was conducted in DA and DB cholinergic motoneurons. *rab-5 Q78L* and *rab-10* mutants displayed defects in secretion. Note: RNAi experiments were normalized to knockdown of mock vector (L4440). [Scale bars: 6 μm (in DNC); 4 μm (in coelomocytes).] At least $n = 10$ animals were tested per strain. Representative images are shown here for DNC (*A*) and coelomocytes (*B*). For quantification, refer to Fig. 1.

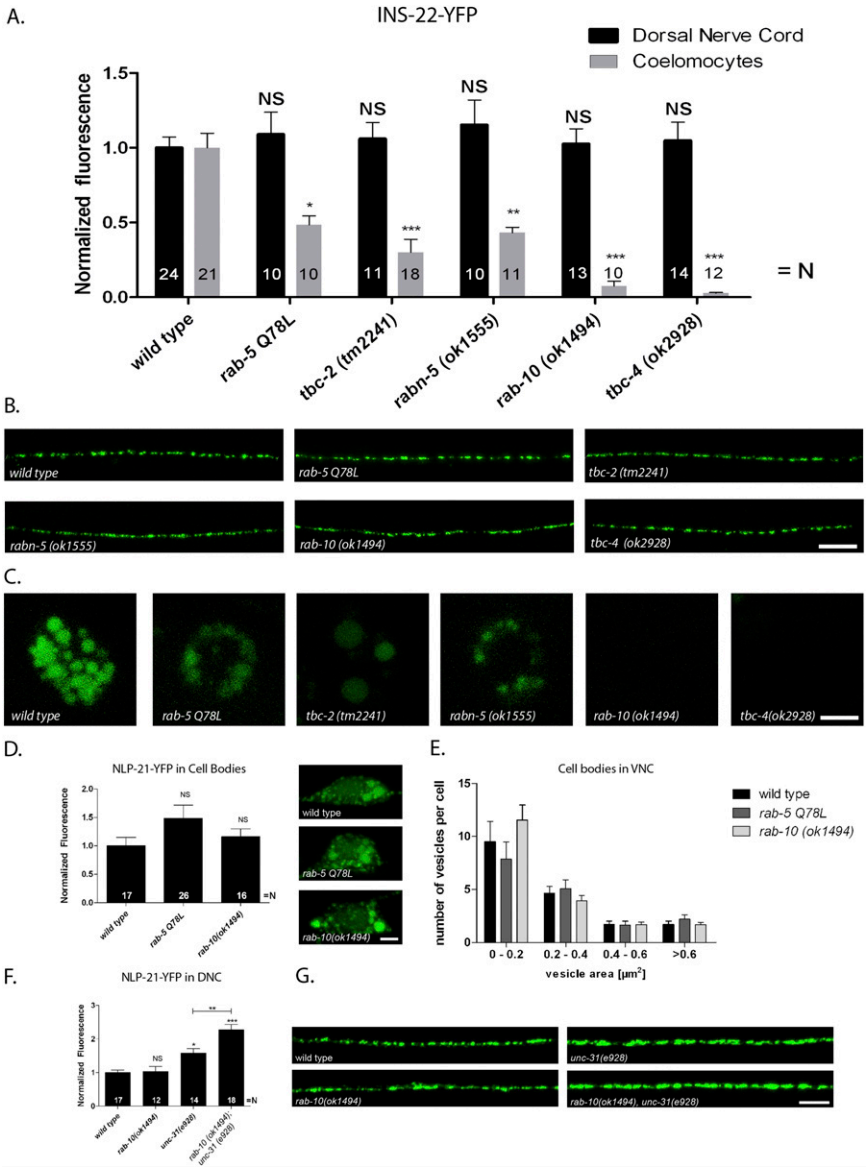

Fig. S2. INS-22-YFP secretion is also decreased in *rab-5 Q78L*, *tbc-2*, *rab-10*, and *tbc-4* mutants. (*A–C*) The secretion of another DCV marker, INS-22-YFP, is also perturbed in *rab-5 Q78L*, *tbc-2*, *rab-10*, *and tbc-4* mutants. [Scale bars: 6 μm (in DNC); 5 μm (in coelomocytes).] Error bars indicate SEM. ***$P < 0.001$; **$P < 0.01$; *$P < 0.05$ (one-way ANOVA with Bonferroni post test). (*D* and *E*) Analysis of NLP-21-YFP levels in cell bodies, as well as sizes of NLP-21-YFP–positive organelles, in cholinergic motoneurons revealed no trafficking defect in *rab*-5 and *rab-10* mutants. (Scale bar: 2 μm.) Error bars indicate SEM (one-way ANOVA with Bonferroni post test). (*F* and *G*) Double mutants of *unc-31* and *rab-10* displayed an increase in DNC fluorescence to levels higher than that observed in *unc-31* mutants. (Scale bar: 5 μm.) Error bars indicate SEM. ***$P < 0.001$; **$P < 0.01$; *$P < 0.05$ (one-way ANOVA with Bonferroni post test).

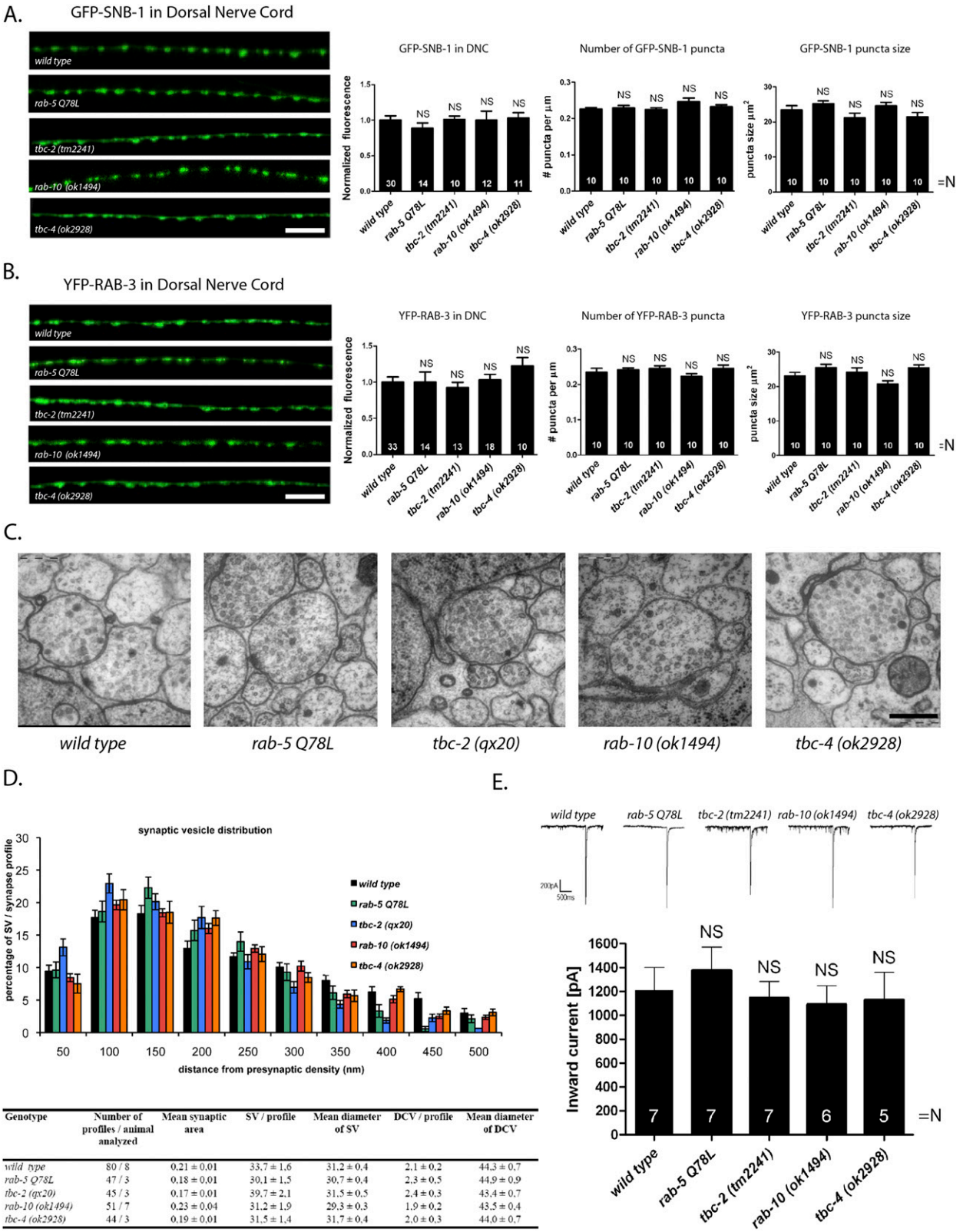

Genotype	Number of profiles / animal analyzed	Mean synaptic area	SV / profile	Mean diameter of SV	DCV / profile	Mean diameter of DCV
wild type	80 / 8	0,21 ± 0,01	33,7 ± 1,6	31,2 ± 0,4	2,1 ± 0,2	44,3 ± 0,7
rab-5 Q78L	47 / 3	0,18 ± 0,01	30,1 ± 1,5	30,7 ± 0,4	2,3 ± 0,5	44,9 ± 0,9
tbc-2 (qx20)	45 / 3	0,17 ± 0,01	39,7 ± 2,1	31,5 ± 0,5	2,4 ± 0,3	43,4 ± 0,7
rab-10 (ok1494)	51 / 7	0,23 ± 0,04	31,2 ± 1,9	29,3 ± 0,3	1,9 ± 0,2	43,5 ± 0,4
tbc-4 (ok2928)	44 / 3	0,19 ± 0,01	31,5 ± 1,4	31,7 ± 0,4	2,0 ± 0,3	44,0 ± 0,7

Fig. S3. Localization, size, distribution, and release of synaptic vesicles is unaffected in *rab-5 Q78L*, *tbc-2*, *rab-10*, and *tbc-4* mutants. Analysis of GFP-SNB-1 (*A*) and YFP-RAB-3 (*B*) showed no change in fluorescence intensities, number of puncta, and puncta size at DNC synapses in *rab-5 Q78L*, *tbc-2*, *rab-10*, and *tbc-4* mutants. [Scale bar; 6 µm (in DNC).] Error bars indicate SEM [not significant (NS), $P > 0.05$; one-way ANOVA with Bonferroni post test]. Ultrastructural analysis of *rab-5 Q78L*, *tbc-2*, *rab-10*, and *tbc-4* mutant synapses revealed no change in synapse morphology (*C*) or the distribution (*D*) of SVs from the presynaptic density. (Scale bar: 400 nm.) Error bars indicate SEM (NS, $P > 0.05$; one-way ANOVA with Bonferroni post test). (*E*) Photo-evoked responses from the NMJ showed no changes in EPSCs in *rab-5 Q78L*, *tbc-2*, *rab-10*, and *tbc-4* mutants. Error bars indicate SEM (NS, $P > 0.05$; one-way ANOVA with Bonferroni post test).

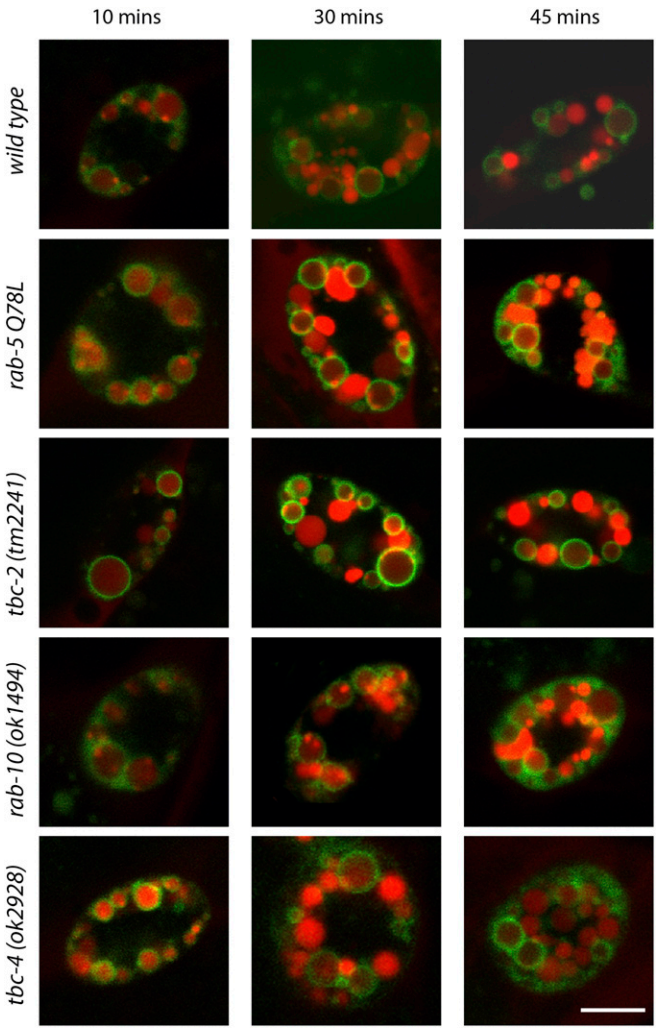

Fig. S4. Analysis of TR-BSA endocytosis in *rab-5 Q78L*, *tbc-2*, *rab-10*, and *tbc-4* mutant coelomocytes. The endocytosis and the kinetics of endocytosis of TR-BSA in the coelomocytes of *rab-5 Q78L*, *tbc-2*, *rab-10*, and *tbc-4* mutants are not affected. RME-8-GFP was used as an early endosomal marker. Red, TR-BSA; green, RME-8-GFP. (Scale bar: 5 μm.)

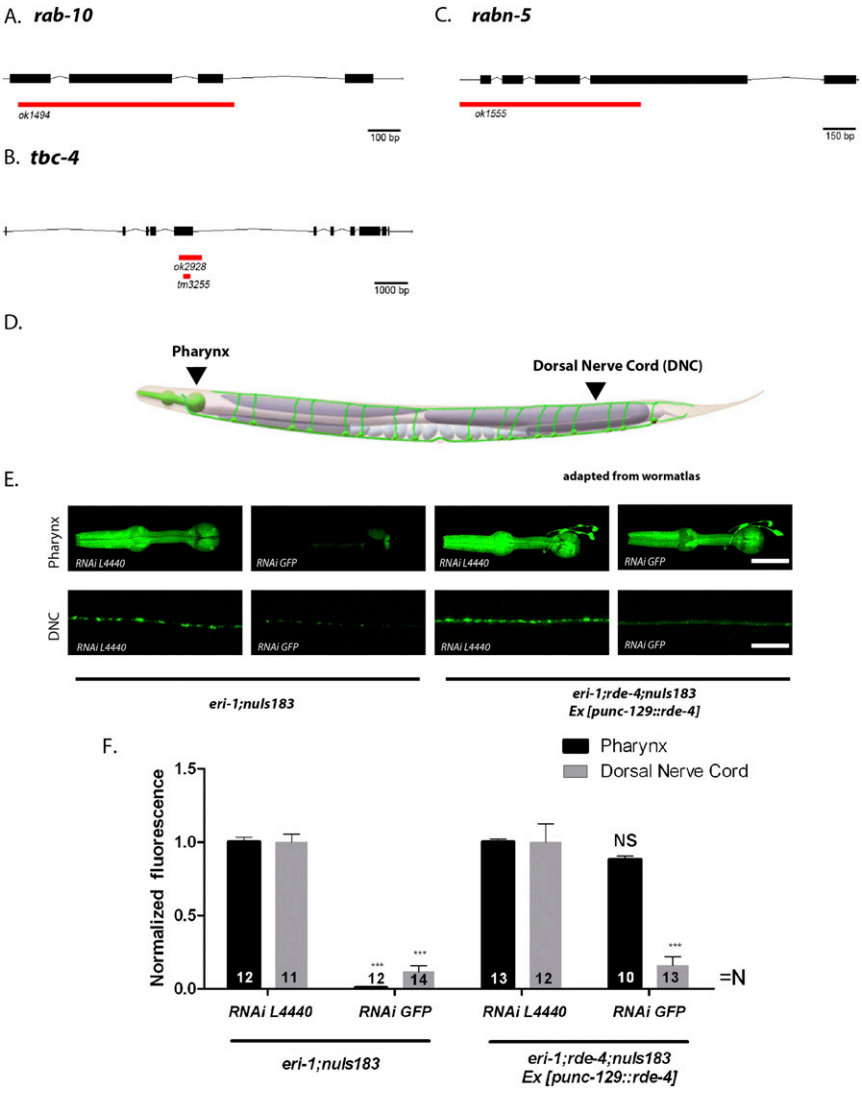

Fig. S5. Gene structures of alleles used in this study and tissue-specific RNAi. The gene structures of *rab-10* (*A*), *tbc-4* (*B*), and *rabn-5* (*C*) are depicted with exons as blocs and introns as lines. Deletion alleles that were used in the study are also described. Red lines indicate the segments of the genes that were deleted for the respective allele. (*D–F*) Validation of tissue-specific RNAi in neurons. Tissue-specific knockdown was achieved by using an RNAi-deficient mutant, *rde-4*, rescued with *rde-4* expression in the DA and DB motoneurons using the *unc-129* promoter. (Note: transgenic animals express the coinjection marker, *pttx-3::gfp*, in head neurons.) This strain, *rde-4 Ex[punc-129::rde-4]*, was crossed into the *eri-1* (for enhanced RNAi sensitivity) and the *nuls183* (NLP-21-YFP assay strain) backgrounds. (*D*) Schematic representation of the tissue specific *eri-1; rde-4;nuis183 Ex [punc-129::rde-4]* RNAi strain. (*E* and *F*) Control experiments knocking down GFP in a nonneuronal tissue (pharynx) vs. DNC in the *eri-1; rde-4; nuls183 Ex[punc-129::rde-4]* strain showed a specific decrease in YFP levels in the DNC (15.89 $\pm$ 6.10%), whereas GFP levels were unaffected in the pharynx. [Scale bars: 50 μm (in pharynx); 6 μm (in DNC).] Error bars indicate SEM. ***$P < 0.001$ (one-way ANOVA with Bonferroni post test).

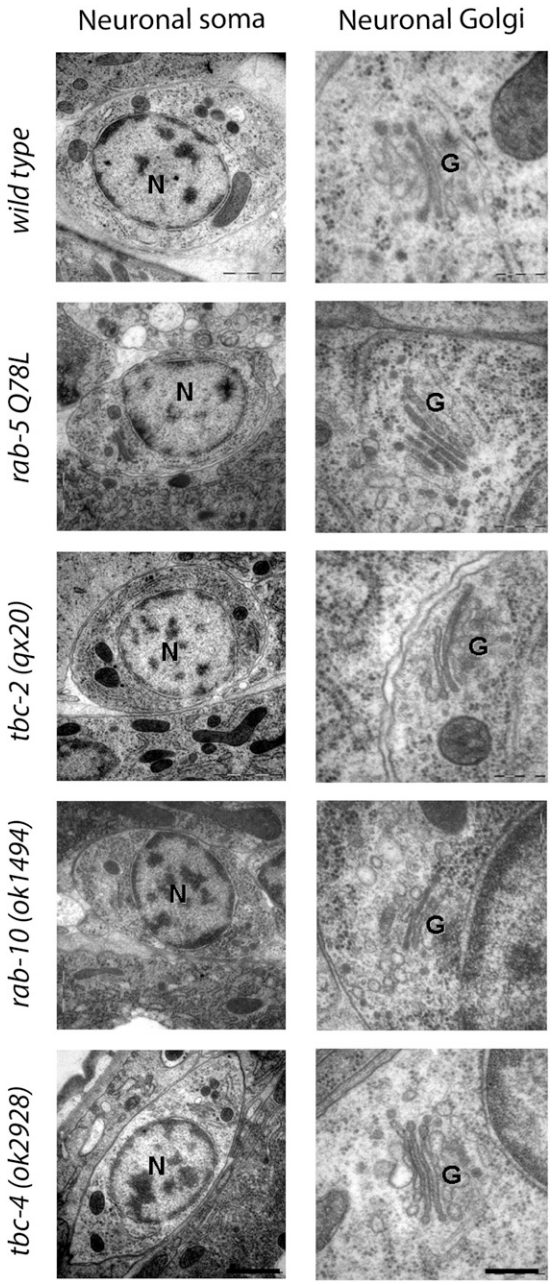

Fig. S6. Morphological analysis of neuronal cell somas and Golgis in *rab-5 Q78L*, *tbc-2*, *rab-10*, and *tbc-4* mutants. Morphological analysis of *rab-5 Q78L*, *tbc-2*, *rab-10*, and *tbc-4* mutant neurons and their Golgis by HPF-EM revealed that were no obvious defects. G, Golgi; N, nucleus. [Scale bars: 1 μm (in somas); 200 nm (in Golgis).]

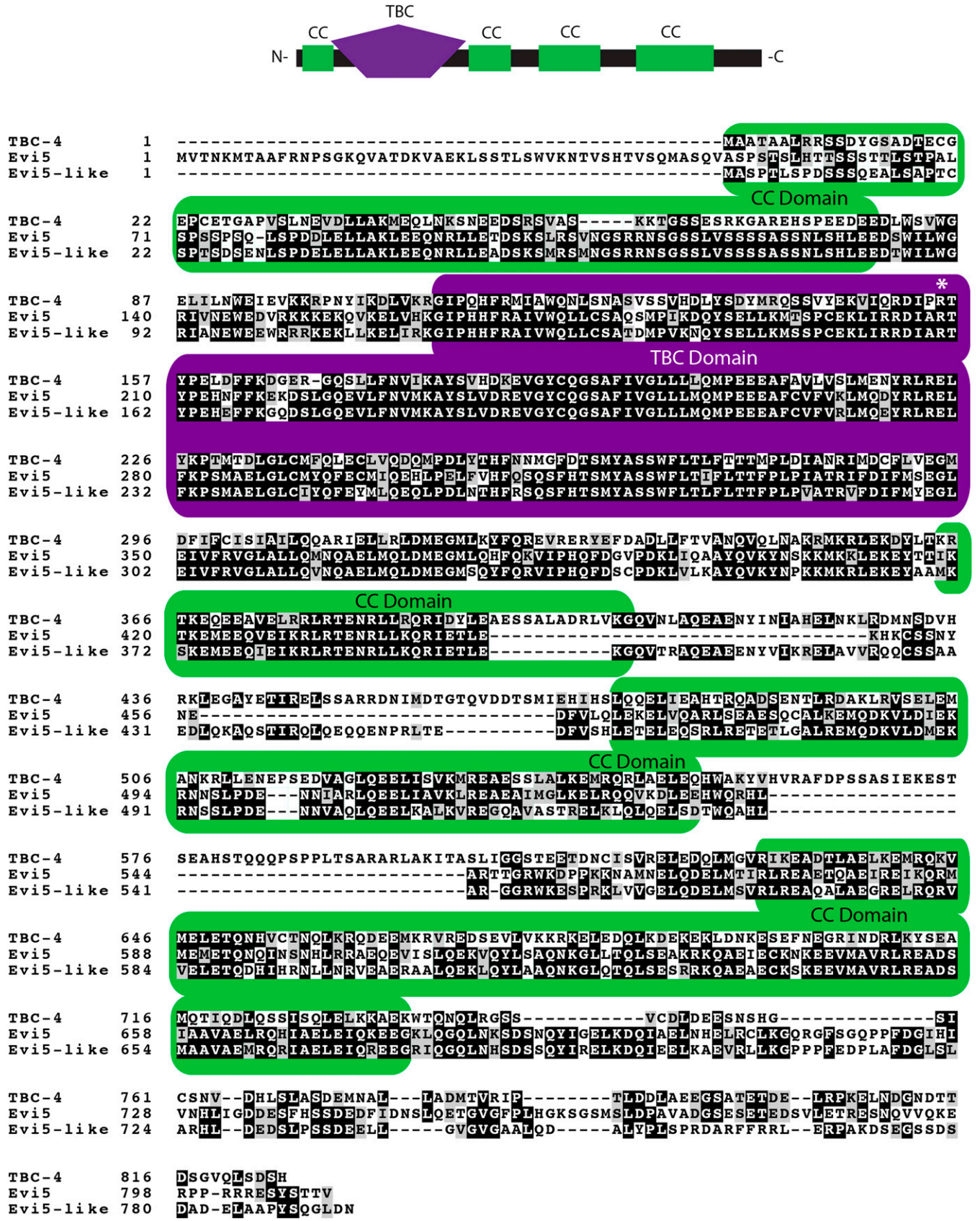

Fig. S7. Multiple sequence alignment of TBC-4 with its human orthologs. Protein sequences of TBC-4 and its closest human orthologs, Evi5 [National Center for Biotechnology Information (NCBI) reference sequence NM_005665] and Evi5-like (NCBI reference sequence NM_001159944), were aligned using MUSCLE. The alignment has been displayed using BOXSHADE. TBC-4 contains one TBC domain (purple) and four CC domains (green). *Conserved catalytic arginine residue, R155, of TBC-4.

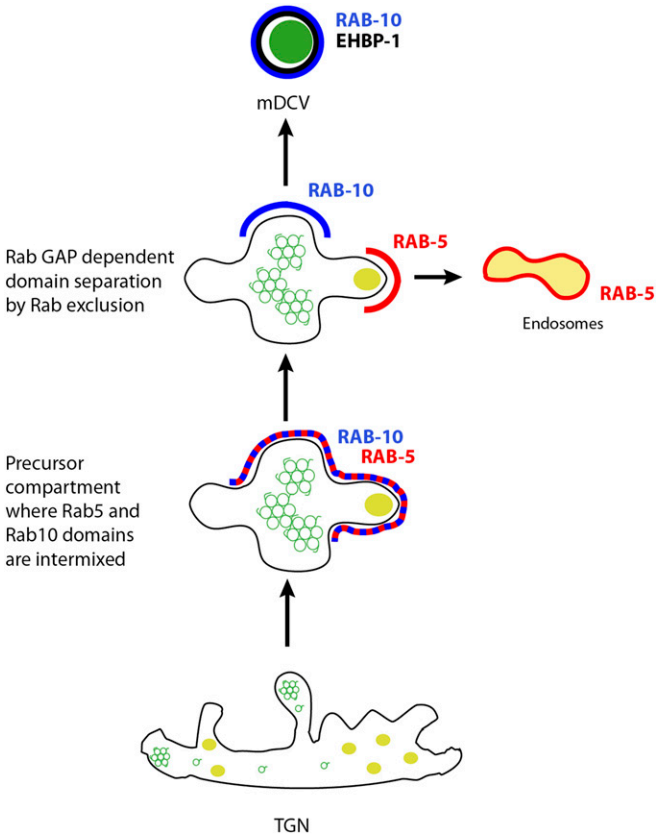

Fig. S8. Model of a RAB-5–RAB-10 exclusion cascade. A schematic representation of the formation of separate RAB-5 and RAB-10 domains from a randomly ordered precursor domain during the formation of mDCVs through a RAB-5–RAB-10 exclusion step. Adapted from (1).

1. Tooze SA, Martens GJ, Huttner WB (2001) Secretory granule biogenesis: Rafting to the SNARE. *Trends Cell Biol* 11:116–122.

Table S1. List of strains used in study

Strain name	Genotype
MT1093	*unc-108 (n501)*
NM791	*rab-3 (js49)*
VC2117	*rab-6.2 (ok2254)*
GQ574	*rab-8 (tm2991)*
VC1026	*rab-10 (ok1494)*
GQ575	*rab-11.2 (tm2081)*
GQ576	*rab-14 (tm2095)*
RB1638	*rab-18 (ok2020)*
RB1537	*rab-19 (ok1845)*
VC1372	*rab-21 (ok1879)*
GQ577	*rab-27 (tm2306)*
RB2484	*rab-28 (ok3424)*
RB1376	*rab-33 (ok1561)*
GQ578	*rab-35 (tm2058)*
GQ579	*rab-37 (tm2089)*
GQ580	*rab-39 (tm2466)*
DA509	*unc-31 (e928)*
GQ581	*tbc-2 (qx20)*
GQ582	*tbc-2 (tm2241)*
VC2256	*tbc-4 (ok2928)*
GQ583	*tbc-4 (tm3255)*
RB1370	*rabn-5 (ok1555)*
GR1373	*eri-1 (mg366)*
WM49	*rde-4 (ne301)*
GQ584	*nuIs183[punc129::nlp-21-venus]*
KP3292	*nuIs152[punc-129::gfp-snb-1]*
KP3931	*nuIs168[punc-129::venus-rab-3]*
GQ585	*nuIs195[punc-129::ins-22-venus]*
GQ586	*ceIs72[punc-129::ida-1-gfp]*
GQ587	*zxIs5[unc-17::chop-2 (H134R)-yfp;lin-15(+)]*
GQ588	*zxIs6[unc-17::chop-2 (H134R)-yfp;lin-15(+)]*
DH1336	*bIs34[prme-8::rme-8-gfp]*
GQ1499	*ceIs59[punc-129::yfp-rab-5]*
GQ153	*gz110[prab-3::mcherry-rab-5 Q78L]; nuIs183[punc-129::nlp-21-venus]*
GQ026	*unc-108 (n501); nuIs183[punc-129::nlp-21-venus]*
GQ445	*rab-3 (js49); nuIs183[punc-129::nlp-21-venus]*
GQ446	*rab-6.2 (ok2254); nuIs183[punc-129::nlp-21-venus]*
GQ447	*rab-8 (tm2991); nuIs183[punc-129::nlp-21-venus]*
GQ448	*rab-10 (ok1494); nuIs183[punc-129::nlp-21-venus]*
GQ449	*rab-11.2 (tm2081); nuIs183[punc-129::nlp-21-venus]*
GQ450	*rab-14 (tm2095); nuIs183[punc-129::nlp-21-venus]*
GQ451	*rab-18 (ok2020); nuIs183[punc-129::nlp-21-venus]*
GQ452	*rab-19 (ok1845); nuIs183[punc-129::nlp-21-venus]*
GQ453	*rab-21 (ok1879); nuIs183[punc-129::nlp-21-venus]*
GQ454	*rab-27 (tm2306); nuIs183[punc-129::nlp-21-venus]*
GQ455	*rab-28 (ok3424); nuIs183[punc-129::nlp-21-venus]*
GQ456	*rab-33 (ok1561); nuIs183[punc-129::nlp-21-venus]*
GQ457	*rab-35 (tm2058); nuIs183[punc-129::nlp-21-venus]*
GQ458	*rab-37 (tm2089); nuIs183[punc-129::nlp-21-venus]*
GQ459	*rab-39 (tm2466); nuIs183[punc-129::nlp-21-venus]*
GQ460	*tbc-2 (qx20); nuIs183[punc-129::nlp-21-venus]*
GQ461	*tbc-2 (tm2241); nuIs183[punc-129::nlp-21-venus]*
GQ462	*tbc-4 (ok2928); nuIs183[punc-129::nlp-21-venus]*
GQ463	*tbc-4 (tm3255); nuIs183[punc-129::nlp-21-venus]*
GQ464	*tbc-2 (tm2241); nuIs152[punc-129::gfp-snb-1]*
GQ465	*tbc-4 (ok2928); nuIs152[punc-129::gfp-snb-1]*
GQ466	*rab-10 (ok1494); nuIs152[punc-129::gfp-snb-1]*
GQ467	*gz110[prab-3::mcherry-rab-5Q78L]; nuis152[punc-129::gfp-snb-1]*
GQ468	*tbc-2 (tm2241); nuIs168[punc-129::venus-rab-3]*
GQ469	*tbc-4 (ok2928); nuIs168[punc-129::venus-rab-3]*
GQ470	*rab-10 (ok1494); nuIs168[punc-129::venus-rab-3]*
GQ471	*gz110[prab-3::mcherry-rab-5Q78L]; nuis168[punc-129::venus-rab-3]*
GQ472	*rab-10 (ok1494); zxIs5[unc-17::chop-2 (H134R)-yfp;lin-15(+)]*

Table S1. Cont.

Strain name	Genotype
GQ473	*tbc-2 (tm2241); zxIs5[unc-17::chop-2 (H134R)-yfp;lin-15(+)]*
GQ474	*tbc-4 (ok2928); zxIs6[unc-17::chop-2 (H134R)-yfp;lin-15(+)]*
GQ475	*gz110[prab-3::mcherry-rab-5Q78L]; zxIs5[unc-17::chop-2 (H134R)-yfp;lin-15(+)]*
GQ476	*tbc-2 (tm2241); nuIs195[punc-129::ins-22-venus]*
GQ477	*tbc-4 (ok2928); nuIs195[punc-129::ins-22-venus]*
GQ478	*rab-10 (ok1494); nuIs195[punc-129::ins-22-venus]*
GQ479	*rabn-5 (ok1555); nuIs195[punc-129::ins-22-venus]*
GQ480	*gz110[prab-3::mcherry-rab-5Q78L]; nuIs195[punc-129::ins-22-venus]*
GQ481	*tbc-2 (tm2241); bIs34[prme-8::rme-8-gfp]*
GQ482	*tbc-4 (ok2928); bIs34[prme-8::rme-8-gfp]*
GQ483	*rab-10 (ok1494); bIs34[prme-8::rme-8-gfp]*
GQ484	*gz110[prab-3::mcherry-rab-5Q78L]; bIs34[prme-8::rme-8-gfp]*
GQ485	*rab-10 (ok1494); ceIs72[punc-129::ida-1-gfp]*
GQ486	*gz110[prab-3::mcherry-rab-5Q78L]; ceIs72[punc-129::ida-1-gfp]*
GQ487	*eri-1 (mg366); rde-4 (ne301)*
GQ488	*eri-1 (mg366); rde-4 (ne301); gz133[punc-129::rde-4]*
GQ489	*rab-10 (ok1494); nuIs183[punc-129::nlp-21-venus]; gz130[punc-129::mcherry–rab-10]*
GQ490	*tbc-4 (ok2928); nuIs183[punc-129::nlp-21-venus]; gz131[prab-3::tagrfp-tbc-4]*
GQ491	*tbc-4 (ok2928); nuIs183[punc-129::nlp-21-venus]; gz132[prab-3::tagrfp-tbc-4 R155A]*
GQ492	*N2; gz134[prab-3::gfp–cb-5; prab-3::mcherry–rab-10]*
GQ493	*N2; gz135[prab-3::gfp-εcop; prab-3::mcherry–rab-10]*
GQ494	*N2; gz136[prab-3::mannosidase II–yfp; prab-3::mcherry–rab-10]*
GQ495	*N2; gz137[prab-3::gfp–2xfyve domain; prab-3::mcherry–rab-10]*
GQ496	*N2; gz138[prab-3::tagrfp-syx-6; prab-3::gfp–rab-10]*
GQ497	*N2; gz139[prab-3::tagrfp-tbc-4; prab-3::gfp-rab-10]*
GQ499	*N2; gz141[prab-3::tagrfp-rabn-5; prab-3::gfp-tbc-4]*
GQ500	*N2; gz142[prab-3::ehbp-1-tagrfp; prab-3::gfp–rab-10]*
GQ501	*N2; gz143[prab-3::yfp-apt-9; prab-3::mcherry–rab-10]*
GQ1498	*nuis152[punc-129::gfp-snb-1]; gz799[punc-129::mcherry-rab-10]*
GQ1499	*nuis168[punc-129::venus-rab-3]; gz799[punc-129::mcherry-rab-10]*
GQ1500	*gzsi1[prab-3::mcherry-rab-10]*
GQ1501	*ceis59[punc-129::yfp-rab-5]; gzsi1[prab-3::mcherry-rab-10]*
GQ1502	*nuIs183[punc-129::nlp-21-venus]; gzsi1[prab-3::mcherry-rab-10]*
GQ1503	*unc-31 (e928); rab-10 (ok1494); nuIs183[punc-129::nlp-21-venus]*
GQ1504	*N2; gz800[prab-3::yfp-rab-5; prab-3::tagrfp-rab-10]*
GQ1505	*tbc-2 (tm2241); gz800[prab-3::yfp-rab-5; prab-3::tagrfp-rab-10]*
GQ1506	*tbc-4 (ok2928); gz800[prab-3::yfp-rab-5; prab-3::tagrfp-rab-10]*
GQ1507	*nuIs183[punc-129::nlp-21-venus]; gz801[prab-3::tagrfp-rab-10 Q68L]*
GQ1508	*nuIs183[punc-129::nlp-21-venus]; gz802[punc-129::tagrfp-rab-5 Q78L]*
GQ1509	*nuIs183[punc-129::nlp-21-venus]; gz803[prab-3::tagrfp-tbc-2]*
GQ1510	*nuIs183[punc-129::nlp-21-venus]; gz804[prab-3::tagrfp-tbc-2 R689A]*
GQ1511	*N2; gz805[prab-3::yfp-tbc-2; prab-3::tagrfp-rab-10 Q68L]*
GQ1512	*N2; gz806[prab-3::yfp-tbc-2; prab-3::tagrfp-rab-10 T23N]*
GQ1513	*N2; gz807[prab-3::yfp-tbc-4; prab-3::mcherry-rab-5 Q78L]*
GQ1514	*N2; gz808[prab-3::yfp-tbc-4; prab-3::mcherry-rab-5 S33N]*

Table S2. List of injection mixes used to generate extrachromosomal arrays

Array name	Plasmid	Markers
gz130	5 ng/μL *punc-129::mcherry–rab-10*	20 ng/μL *prab-28::tagrfp*
gz131	20 ng/μL *prab-3::tagrfp-tbc-4*	20 ng/μL *pttx-3::gfp*
gz132	20 ng/μL *prab-3::tagrfp-tbc-4 R155A*	20 ng/μL *prab-28::tagrfp*
gz133	20 ng/μL *punc-129::rde-4*	20 ng/μL *pttx-3::gfp*; 40 ng/μL *pRF4(rol-6(su1006))*
gz134	10 ng/μL *prab-3::gfp–cb-5*; 3 ng/μL *prab-3::mcherry–rab-10*	40 ng/μL *pRF4(rol-6(su1006))*
gz135	10 ng/μL *prab-3::gfp-εcop*; 3 ng/μL *prab-3::mcherry–rab-10*	40 ng/μL *pRF4(rol-6(su1006))*
gz136	10 ng/μL *prab-3::mannosidase II–yfp*; 3 ng/μL *prab-3::mcherry–rab-10*	40 ng/μL *pRF4(rol-6(su1006))*
gz137	10 ng/μL *prab-3::gfp–2xfyve domain*; 3 ng/μL *prab-3::mcherry–rab-10*	40 ng/μL *pRF4(rol-6(su1006))*
gz138	3 ng/μL *prab-3::tagrfp-syx-6*; 3 ng/μL *prab-3::gfp–rab-10*	30 ng/μL *pRF4(rol-6(su1006))*
gz139	20 ng/μL *prab-3::tagrfp-tbc-4*; 3 ng/μL *prab-3::gfp-rab-10*	30 ng/μL *pRF4(rol-6(su1006))*
gz141	15 ng/μL *prab-3::tagrfp-rabn-5*; 20 ng/μL *prab-3::gfp-tbc-4*	30 ng/μL *pRF4(rol-6(su1006))*
gz142	20 ng/μL *prab-3::ehbp-1-tagrfp*; 5 ng/μL *prab-3::gfp–rab-10*	20 ng/μL *pttx-3::gfp*
gz143	20 ng/μL *prab-3::yfp-apt-9*; 5 ng/μL *prab-3::mcherry–rab-10*	20 ng/μL *pttx-3::gfp*; 30 ng/μL *pRF4(rol-6(su1006))*
gz799	5 ng/μL *punc-129::mcherry-rab-10*	2.5 ng/μL *pmyo-2::mcherry*
gz800	3.5 ng/μL *prab-3::yfp-rab-5*; 3.5 ng/μL *prab-3::tagrfp-rab-10*	40 ng/μL *pRF4(rol-6(su1006))*; 20 ng/μL *pttx-3::gfp*
gz801	5 ng/μL *prab-3::tagrfp-rab-10 Q68L*	40 ng/μL *pRF4(rol-6(su1006))*; 20 ng/μL *pttx-3::gfp*
gz802	10 ng/μL *punc-129::tagrfp-rab-5 Q78L*	40 ng/μL *pRF4(rol-6(su1006))*; 30 ng/μL *pttx-3::gfp*
gz803	20 ng/μL *prab-3::tagrfp-tbc-2*	—
gz804	20 ng/μL *prab-3::tagrfp-tbc-2 R689A*	—
gz805	20 ng/μL *prab-3::yfp-tbc-2;* 5 ng/μL *prab-3::tagrfp-rab-10 Q68L*	40 ng/μL *pRF4(rol-6(su1006))*
gz806	20 ng/μL *prab-3::yfp-tbc-2;* 5 ng/μL *prab-3::tagrfp-rab-10 T23N*	40 ng/μL *pRF4(rol-6(su1006))*
gz807	20 ng/μL *prab-3::yfp-tbc-4;* 5 ng/μL *prab-3::mcherry-rab-5 Q78L*	40 ng/μL *pRF4(rol-6(su1006))*
gz808	20 ng/μL *prab-3::yfp-tbc-4;* 5 ng/μL *prab-3::mcherry-rab-5 S33N*	40 ng/μL *pRF4(rol-6(su1006))*

Dashes indicate translational fusions.